RSC Advances

ROYAL SOCIETY OF CHEMISTRY

www.rsc.org/advances

Cite this: DOI: 10.1039/c0xx00000x

www.rsc.org/xxxxxx

ARTICLE TYPE

Analysis of bimodal thermally-induced denaturation of type I collagen extracted from calfskin

Teodora Staicu,[a] Viorel Cîrcu,[b] Gabriela Ioniţă,[c] Corneliu Ghica,[d] Vlad T. Popa*[,c] and Marin Micutz*[,a,c]

Received (in XXX, XXX) Xth XXXXXXXXX 20XX, Accepted Xth XXXXXXXXX 20XX

DOI: 10.1039/b000000x

The most widely occurring collagen in the extracellular matrix of the mammalian tissues – type I collagen has attracted a huge interest from both theoretical and practical points of view. The results presented herein are mainly confined to a study on the thermal stability of type I collagen (CI) extracted from calfskin in acidic solutions (10^{-2}M HCl). A two-step process associated to the heat-induced denaturation of CI was revealed by using ultra sensitive differential scanning calorimetry. The minor endothermic transition (peak temperatures of about 30.5-30.8^{0}C) has been assigned to the defibrillation of small supramolecular CI assemblies (occurring in solution) while the major endothermic transition (about 34.8-35.0^{0}C) has been ascribed to denaturation of CI, consisting in a complete unfolding of the native triple-helical conformation of the collagen molecule. The calorimetric data were supported by information obtained from capillary viscometry performed on the same solutions. The native state of CI (molecular integrity and triple-helical conformation) for all the systems studied in this paper was confirmed by transmission electron microscopy, ultraviolet circular dichroism and capillary viscometry. At the same time, based on the sodium dodecyl sulphate-polyacrylamide gel electrophoresis and an appropriate image processing of the corresponding electropherogram, a certain degree of intramolecular crosslinking of CI was detected, mainly between α1 and α2 chains of the collagen triple-helix. Such a feature seems to be caused by both the nature of the extraction procedure and the storage conditions.

Introduction

Of the 28 collagen types identified in human body and more than 50 collagens and collagen-like proteins in mammalian kingdom, the type I collagen (CI) is the most widely occurring collagen in the connective tissues of the vertebrates.[1-3] As in the case of all collagens, the primary structure of CI contains the repeating amino acid structure (Gly-X-Y), where X and Y can be any α-amino acid residue, most frequently proline and hydroxyproline residues, respectively.[1,4] CI belongs to the so-called fibrillar collagens, together with other members (especially of type II and III), and has a long and uninterrupted triple-helical conformation consisting of three individual α-chains. Each of them contains ca. 330 (Gly-X-Y) units and forms left-handed poly-L-proline II (PPII) helical arrangement. The three α-chains are twisted around each other into a right-handed superhelix (called triple-helix) which is the central part of the CI molecule.[1-4] From the chain composition standpoint, the CI molecules, as they are spread in extracellular matrix of the connective tissues, are heterotrimers, $[\alpha1(I)]_2\alpha2(I)$, with two identical α1 polypeptide chains and another distinct α2 chain. At molecular level, in the native state, CI still contains two short non-triple-helical regions (called C- and N-telopeptides), each covalently bound at both triple-helix ends, playing an essential role in collagen fibrillogenesis.[2,5] This entire molecular structure is referred to as tropocollagen (type I tropocollagen, in this case) having approximately 300 nm in length and 1.5 nm in diameter.[2,6,7] Based on a pronounced biomechanical function (due to its ability to assembly in fibrils) into the tissues where it is located, the CI is the main subject in a lot of scientific research for many decades, most of attention being focused on its usefulness as a biomaterial, in tissue engineering or as drug-delivery systems. Thus, these manifold utilities of CI are highly illustrated in fabrication of biomimetic collagen-apatite scaffolds or collagen biomineralization,[8-14] in designing some collagen-based scaffolds for soft tissues regeneration,[15,16] as biomaterial useful in preparation of three-dimensional matrices suited for various applications (as crosslinked collagen hydrogels,[17] drug-delivery systems with a particular architecture,[18] 3D neural extracellular matrix[19] or 3D brain model[20] in studying certain wound healing, soft/hard tissue regeneration, regeneration of neurites or tumour cell migration processes, respectively) or in thin layer/multilayer deposition onto flat surfaces, with highly oriented arrays of collagen molecules resulted by either quasi-epitaxial growth[21] or Langmuir-Blodgett technology.[22,23] Last but not least, almost all these practical applications involve collagen as supramolecular aggregates that requires knowing the mechanism, microstructure and actual conditions of collagen fibril formation.[24,25] At the same time, any application of CI or CI-based systems such as those just mentioned also requires preliminarily knowledge on the collagen stability both at molecular and supramolecular level under the

actual conditions of practical purposes: temperature, pH, ionic strength, concentration/water content or mechanical loading behaviour. One of the most important features having a great influence onto behaviour of collagen or collagen-based systems is its thermal stability. Many earlier and recent studies dedicated to this topic show that the CI with a native conformation experiences a helix-coil transition as temperature increases. Temperature at which this transition occurs (denaturation temperature) typically rises as the degree of collagen hydration (that may set physical state) decreases.[26-28] In fact, such a thermal denaturation of CI was considered to be a rather sharp transformation of triple-helical structure into a random-coil one, which is a type of conformation that implies a totally random distribution of the α-amino acid residues within sterically-allowed domains of the Ramachandran plot.[29] A number of investigations on protein/polypeptide unfolding show that what has normally been believed to be a random-coil is practically a conformational structure that preserves a certain extent of PPII arrangement within short ranges belonging to the macromolecular chain. These subtle findings regarding the local conformation of so-called random coil were revealed mainly by ultraviolet circular dichroism (UV-CD),[30-32] vibrational circular dichroism (VCD)[33] or both.[27] A comprehensive treatment on PPII and random-coil conformation was reviewed by Bochicchio and Tamburro[34] and, recently, by Adzhubei *et al*.[35] In accordance with these studies, in order to avoid any confusion derived from the resemblance between local PPII arrangement and random-coil conformation, instead of the terminology "helix-coil transition" induced by heating, "helix-unordered state transition" should be considered. Depending on the particular physical state of collagen-based systems, the assessment of collagen stability upon heating and associated conformational changes assume suitable techniques to be employed: viscometry, differential scanning calorimetry (DSC), infrared spectroscopy (FTIR)/Raman spectroscopy, UV-CD, VCD - for liquid state and DSC, FTIR/Raman spectroscopy, UV-CD, VCD - for solid state. The fact that the living cell functioning is strongly related to the liquid state (solution or aqueous dispersions whereby the majority of physiological processes occur) accounts for the interest of studying thermal stability of collagen in solution or aqueous dispersion state. In this respect, a lot of research revealed a two-stage character of the CI thermal denaturation both in acidic solutions and aqueous dispersions. An overall analysis of the published results seems to outline two dominant explanations.

Firstly, the bimodal behaviour of the heat induced denaturation of CI is related to the simultaneous presence of two types of collagen structures: monomeric collagen (distinct molecules of collagen) and collagen fibrils/microfibrils. From this point of view, based on DSC investigations, some authors assigned the low-temperature endothermic peak to the melting (unfolding) of monomeric collagen, while the high-temperature peak was considered to originate from collagen fibril/microfibril denaturation under fibril-forming conditions.[36] The same results have been also obtained by Danielsen[37] by using UV spectroscopy (absorption difference, recorded at 227 nm, between the identical sample and reference aqueous collagen dispersions during the sample heating). Other investigators stated that the endothermic peak located at lower temperature can be related to the collagen defibrillation and the peak placed at higher temperature is caused by monomeric collagen denaturation.[38] Furthermore, Liu *et al*. concluded that the minor thermal transition occurring at lower temperature is determined by both defibrillation of smaller collagen fibrils and partial unfolding of CI molecules, whereas the major endothermic peak comes from the simultaneous processes of defibrillation of larger collagen fibrils and denaturation of the entire collagen triple-helix.[39]

Secondly, such a two-step process of collagen denaturation has been explained taking into account the occurrence of two relatively different domains along the CI molecule.[40] These two different thermally stable regions of CI are considered to be rich-hydroxyproline (Hyp) (with high stability and denaturation temperature) and deficient-Hyp (more labile and lower denaturation temperature), respectively; that was supported by the well-known stabilization effect of Hyp residues on the triple-helix stability of collagen or collagen-like polypeptides when they are basically located in the Y position of the repeating triplet (Gly-X-Y).[41-44]

Within the framework of these controversial debates on the bimodal denaturation of CI, especially upon the acidic conditions, the present contribution is focused on heat-induced denaturation of calfskin CI in aqueous acidic solution based on ultra-sensitive MicroDSC investigations. At the same time, some peculiar related aspects (purity, molecular integrity, intramolecular crosslinking, flow behaviour) are critically analyzed based on the complementary information revealed by TEM, capillary viscometry, UV-CD and SDS-PAGE.

Experimental

Chemicals and reagents

Sodium dodecyl sulphate (SDS, ≥99%), acrylamide (≥99%), bis-acrylamide (N,N'-methylenebisacrylamide, ≥99%), Tris-HCl (Trisma hydrochloride, ≥99%), N,N,N',N'-tetramethylethylenediamine (TEMED, ≥99%) – from Fluka-BioChemika, glycine (≥99%) – from Fluka Analytical, 2-mercaptoethanol (≥99%), Tris [Tris(hydroxymehyl) aminomethane, ACS reagent, 99.8+%], CaO (powder, ReagentPlus, >99.9%), ammonium persulphate (AP, 98%), bromophenol blue (Reag. ACS), trans-4-hydoxy-L-proline (Hyp, ≥99%), Ehrlich's reagent [4-(N,N-dimethylamino)benzaldehyde, ≥99%], chloramine-B (N-chloro-4-benzenesulfonamide sodium salt, ≈28% active chlorine bases), ethyl cellosolve (99%), perchloric acid (ACS reagent, 60%), trifluoroacetic acid (ReagentPlus, 99%), pepsin (from porcine gastric mucosa, >400 units/mg protein) – from Sigma-Aldrich and Brilliant Blue R (pure) – from ACROS ORGANICS were used without further purification. The other chemicals and reagents were purchased from CHIMOPAR SA (Bucharest, Romania) and used as received.

Extraction and purification of collagen

CI was extracted from calfskin (acquired from SC Ladrisi Group SRL, Prahova, Romania via SC Taro Comimpex SRL, Bucharest, Romania) by limited pepsin digestion, then separated and purified by salting out procedures, adjusting the methods described elsewhere.[45-47] Thus, to an amount of freshly shaved six-month-old calfskin (100 g), a corresponding volume of liming mixture

(1.5 g Na_2S, 5 g CaO and distilled water up to overall volume of 200 mL) was added and kept under intermittent stirring for 2 days. To complete this unhairing step, a subsequent deliming process was performed (by adding 2 g NH_4Cl and ca. 4 mL concentrated HCl to the previous system followed by an extensive rinsing with distilled water). The calfskin so-treated was then cut into very small pieces and submerged into 10 volumes of aqueous 0.1M NaOH solution for 24 h, stirring every now and then to remove the non-collagenous proteins. After washing with cold water (ca. 5^0C) until neutral pH of wash water was achieved, the alkali-treated calfskin has been defatted by use of 10 volumes of 10% aqueous solution of butanol (24 h, with butanol solution changed every 6 h). To completely remove the butanol traces, the calfskin pieces were rinsed with a suitable amount of cold distilled water several times. The collagen extraction itself implies soaking the calfskin in 30 volumes of 0.5 M acetic acid containing 1% pepsin (with respect to dry calfskin) for 2 days under discontinuous stirring. After that, the mixture was filtered through two layers of cheese cloth. The filtrate mainly containing type I tropocollagen was clarified by centrifugation (10,000×g) for 20 min and then the collagen are salted out by adding NaCl powder to a final concentration of 3M. Collagenous precipitate was separated by centrifugation (10,000×g for 20 min) and dissolved afterwards in a large enough volume of 0.5M acetic acid. This step was followed by a similar salting out (to a final NaCl concentration of 0.7M) – centrifugation (10,000×g for 20 min) – precipitate dissolution (0.5M acetic acid) sequence to obtain an acetic solution of quite pure CI (as type I tropocollagen). Further purification of CI requires an extensive dialysis of the CI acidic solution against Tris buffer (pH 7.4 using a mixture of Tris and Tris-HCl adjusted with HCl or NaOH; 0.3M NaCl). Maintaining the pH at 7.4, the possibly present type III collagen was removed by its precipitation in 1.7M NaCl solution. The supernatant resulted after centrifugation was subjected to a salting out of CI by 2.5M NaCl solution. The precipitate of CI separated by centrifugation was again dissolved in 0.5M acetic acid solution and subsequently dialyzed against 0.1M acetic acid. The acetic acid solution of pure CI was eventually freeze-dried and lyophilized CI was kept at -20^0C. The CI solutions investigated in the present study were obtained from a CI stock solution (ca. 1% w/v) freshly prepared by dissolution of a corresponding weight of lyophilized CI into a proper volume of HCl 10^{-2}M under a gentle stirring overnight. All the experimental procedures above described have been performed within a temperature range of 2-8^0C to maintain the native triple-helix structure of CI.

Transmission electron microscopy (TEM)

In an attempt to visualize CI at molecular scale, TEM study was performed onto suitable samples through replica casting in the version known as mica sandwich-rotary shadowing technique. A detailed presentation of the method may be found in some earlier studies.[48-53] Briefly, the principle of this type of sample preparation consists of the adsorption of macromolecules onto a mica surface (atomically smooth surface) followed by a heavy-metal (Pt, Au, Pd, Cr) deposition (through evaporation induced by resistive heating of a tungsten filament under high vacuum) while the mica surface spins with 1-2 rot/sec. To provide for more stability and conductivity of the deposited metal film, graphite evaporation (by electric arc) is needed and then carbon-metal replica is removed from the mica substrate and carefully placed onto a copper grid for exposure to the electron beam. Enhancement of the contrast within the surface portions which macromolecules are adsorbed on requires that metal deposition to be carried out at incident angles less than or close to 10^0. In this instance, metal deposition has been made at an incidence angle of 5^0 by use of chromium (99.99%) and employing a high vacuum evaporator JEOL JEE 4C (5×10^{-6} torr). Prior to the chromium and carbon deposition step, a droplet of CI solution (≈5 μL) was placed between the two freshly cleaved mica surfaces resulting in a sandwich packing with a solution middle layer of 10 μm thick.[48] A uniform distribution of the CI molecules adsorbed onto the mica substrate is considerably improved when the collagen solution contains anhydrous glycerine to a final volume concentration of 70%.[48,49] Moreover, an appropriate concentration of CI is required to assure a certain surface density of macromolecules. Thus, based on the particular mica sandwich packing, a CI solution (in acetic acid 0.1M and glycerine – 70%) of 1.5×10^{-4}% (w/v) was used to reach an expected surface density of ca. 15 collagen molecules/μm^2.[48,53] Completely drying of the mica substrates wetted by collagen solution took place inside the same chamber of the high vacuum evaporator JEOL JEE 4C for 3 h. TEM examination of replicas so prepared was performed on electron microscope JEOL TEMSCAN 200CX at the acceleration voltage of 200 kV.

Ultraviolet circular dichroism (UV-CD)

The UV-CD technique was employed for assessing the native triple-helix arrangement of CI in acidic solution. Accordingly, a CI solution of 0.10% (w/v) was prepared in 10^{-2}M HCl. UV-CD spectra were acquired by means of spectropolarimeter Jasco J-810 with a square quartz cuvette (Suprasil, path length 0.10 cm) for UV domain and the following operating parameters: wavelength range 250-190 nm; scanning speed of spectra - 50 nm/min with 0.2 nm pitch; number of spectra acquisition - 4; temperature - room temperature (23^0C); proper flow injection of nitrogen (purity 99.9995%) to eliminate the interference of oxygen absorption within wavelength range 210-190 nm.

Capillary viscometry

Viscosity measurements were made by using a suspended-level viscometer (Ubbelohde type, SCHOTT, Mainz) with a capillary constant of 0.009056 mm^2/s^2. The flow times were automatically determined by the Viscosity Measuring Unit Viscoclock (an electronic device interfaced to PC) with an accuracy of ±0.01 s. All the capillary viscosity measurements at different temperatures were conducted onto thermostated systems (30 min for each temperature measured with an accuracy of ±0.1^0C) and performed in triplicate. The experimental errors (expressed as relative standard deviations) of viscosities values were less than 1%.

Sodium dodecyl sulphate-polyacrylamide gel electrophoresis (SDS-PAGE) of collagen

SDS-PAGE was performed generally by obeying the Laemmli protocol[54] for evaluation of both purity and molecular mass of the CI extracted from calfskin. The first step in SDS-PAGE experiment is the sample denaturation. In this respect, 0.3 mL of collagen stock solution (1%) were mixed with 100 μL 2-

mercaptoethanol and 1.6 mL sample buffer (66 mM Tris-HCl – pH=6.8, 2% SDS, 10% glycerine and 2.5×10^{-2}% bromophenol blue), enclosed into a sealed vial and heated at 95-96^{0}C for 10 min. In conducting SDS-PAGE, we used a SDS-Laemmli Mini gel system with 10 cm × 8 cm gel cassettes and prepared the two types of polyacrylamide gels: resolving gel of 6% (overall volume 20 mL: aqueous solution of acrylamide 30% and bis-acrylamide 1.5% - 4 mL, Tris-HCl solution of 1.5M and pH 8.8 – 5 mL, SDS solution of 10% - 200 µL, freshly prepared AP solution of 10% - 100 µL, TEMED - 20 µL and water up to total volume of 20 mL) and stacking gel of 3% (final volume 10 mL: aqueous solution of acrylamide 30% and bis-acrylamide 1.5% - 1 mL, Tris-HCl solution of 0.5M and pH 6.8 – 1 mL, SDS solution of 10% - 100 µL, freshly prepared AP solution of 10% - 70 µL, TEMED - 20 µL and water up to total volume of 10 mL). Thus, 5 µL of denatured collagen solution were loaded onto the stacking gel and subjected to electrophoresis at a constant voltage of 200 V using a power supply unit Consort EV233. Together with the sample, the same amount of molecular mass reference standards (SigmaMarker, wide range, molecular mass 6,500-200,000 Da) was also subjected to SDS-PAGE in order to estimate the molecular mass of CI. To visualize protein migrations, the separating gel was stained with an aqueous mixture composed of Brilliant Blue R (0.2%), methanol (20%) and glacial acetic acid (10%) and then destained by an aqueous solution of methanol (20%) and glacial acetic acid (10%). Finally, the pattern of blue protein bands displayed onto a relatively clear background was scanned with an appropriate resolution in grayscale mode and then digitally processed by Origin 8.1 Software.

Determination of collagen concentration

Collagen concentration was estimated from hydroxyproline content according to the method of Ignat'eva *et al*.[55] and supposing that CI contains ca. 13% (by weight) hydroxyproline residues.[55-57] Shortly, after CI was completely hydrolyzed (using a mixture of concentrated hydrochloric and trifluoroacetic acid in a volume ratio of 2:1, at 166^{0}C for 25 min), the resulted hydroxyproline was selectively oxidized with Chloramine-B and the excess of Chloramine-B was decomposed by using perchloric acid. Then, the intensely coloured product resulted from the reaction between the oxidized hydroxyproline (pyrrole ring-containing compound) and Ehrlich's reagent (dissolved in ethyl cellosolve) was spectrophotometrically (absorbance at 557 nm) analyzed based on a proper calibration curve (absorbance at 557 nm vs. hydroxyproline content).

Calorimetric measurements

Thermally induced denaturation of CI in acidic solutions was performed employing a Setaram Differential Scanning Microcalorimeter MicroDSC VII Evo. The instrument was Joule effect factory calibrated and periodically checked with the provided naphthalene standard. The outer thermostating loop was provided by a Julabo F32-HE device operating in standard mode. 3D sensor protection was achieved by purging Nitrogen gas (99.9999%, SIAD - TP). The Calisto v1.077 software package was used for data acquisition and primary signal processing. This included baseline integration and export in Excel with evenly spaced time increments. Heat values obtained were further processed in Excel and Origin 8.1. Exported baselines and thermograms were eventually processed in PeakFit v.4.12 (Systat). Detailed description of data processing is given elsewhere.[58-61] Four CI solutions of concentration 0.075%, 0.100%, 0.220% and 0.290% were prepared from the initial stock solution (1.050% based on hydroxyproline determination) by appropriate dilution with HCl 10^{-2}M. Then, the final acidic solutions of CI were degassed and kept overnight at 4-5^{0}C. An amount of degassed collagen solution (ca. 500 mg) of known concentration was placed in a 1mL cell of Removable Batch type (made of Hastelloy C). Another cell with the same amount of HCl 10^{-2}M was used as a corresponding reference. Sample and reference cells were inserted inside their individual compartments of the microcalorimeter and equilibrated at the initial temperature for 1 h before the onset of heating process. Each sample was heated from 5 to 60^{0}C with five different heating rates (Hr): 0.1, 0.2, 0.3, 0.4 and 0.5 Kmin^{-1}, respectively. The enthalpy changes (ΔH) during the CI denaturation were calculated from the peak area taking into account only the first scan of the thermograms due to the transition irreversibility.

Results and discussion

Prior to MicroDSC analysis of collagen samples, an initial prerequisite is to assess the native molecular integrity and also purity of CI.

Evaluation of the native state and purity of CI extracted from calfskin

To assess the native integrity of collagen triple-helix, we provided evidence for both the geometrical size of CI molecule and its natively triple-helical folded conformation. This was achieved by means of TEM and UV-CD, respectively, utilised as reliable experimental methods.

TEM evidence

As it can be seen in the corresponding micrograph (Fig. 1), CI molecules appear as rod-shaped structures with an average length of 280 nm. This is in a very good agreement with the data quoted in previous studies concerning the triple-helix size of fibril-forming collagens: 988-1018 tripeptide units[6] which are equivalent to a superhelix of 250-300 nm in length and 1.5 nm in diameter.[2,6,7,62-64]

UV-CD results

The native triple-helical conformation of CI in solution may be easily and precisely assessed by UV-CD. This is because the

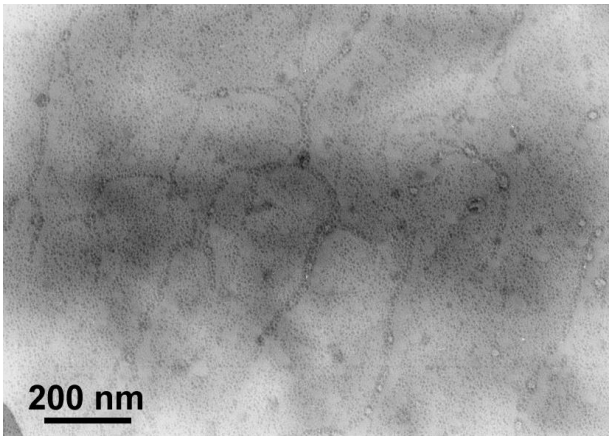

Fig. 1 TEM image at molecular scale for CI.

chirality of such overall α-chains folding results in a secondary structure that resembles the left-handed poly-L-proline II helical arrangement. So, for the native collagen triple-helix there are some peculiar features revealed by the UV-CD spectra: a pronounced negative peak placed within 190-200 nm, a weak positive maximum at ca. 220 nm and a crossover point located around 212 nm.[46,53,65,66] At the same time, an important quantity derived from UV-CD spectra of CI (in acidic solution) is the absolute value of the ratio between the intensity of the positive peak and that of the negative one (Rpn), which is a measure of the helicity degree of the collagen secondary structure.[67,68] Thus, CI in the native conformation in acidic solution is characterized by an Rpn of ca. 0.12.[69] In a very good agreement to these data, the UV-CD spectrum of CI used in this study revealed the following characteristics: positive maximum – 221 nm, negative minimum – 196.6 nm, crossover point – 214 nm, Rpn – 0.12 (Fig. 2). As a consequence, both TEM and UV-CD results fully confirmed the native state of the CI extracted from calfskin according to the procedure described in the experimental section.

Capillary viscometry evaluation

A complementary, reliable and quite accessible experimental approach to establish the molecular integrity of CI in solution is the determination of CI reduced viscosities through capillary viscometry and then the estimation of its intrinsic viscosity. The last quantity may eventually lead to the average viscosity molecular mass ($\overline{M}_v$) of CI in solution. Generally, the reduced viscosity (η_{red}) of a polymer solution obeys a linear dependence against solute concentration according to the well-known Huggins's relationship:[70]

$$\eta_{red} = \frac{\eta_{sp}}{c} = [\eta] + k_H[\eta]^2 c \quad (1)$$

where η_{sp} is the specific viscosity of solution, k_H – the Huggins constant (dimensionless), *[η]* – the intrinsic viscosity of polymer in solution and *c* – polymer concentration in g/dL. Based on the Huggins's equation, *[η]* is the intercept value of the linear dependence η_{red}-c.

The intrinsic viscosity is related to the average viscosity molecular mass of polymer by the so-called Mark-Houwink-Sakurada equation:[71]

$$[\eta] = K(\overline{M}_v)^a \quad (2)$$

where *K* (in dL/g) and *a* (dimensionless) are two constant quantities strongly dependent on the nature of polymer-solvent pair and temperature. For CI, the two constants, determined in 0.15M acetic acid solution at 24.8^{0}C, have the following values: $K=1.23\times10^{-9}$ dL/g and a=1.80.[72,73]

By conducting the capillary viscosity measurements under the abovementioned experimental conditions, a value of 3.59×10^5 Da for the average viscosity molecular mass of CI has been obtained (Fig. 3). Taking into account the 338 amino acid triplets that built each α-chain of CI triple-helix[6] and the 1012 triplets contained into the CI triple-helical domain according to the 3n-2 rule (n is the number of amino acid triplets per α-chain),[4] the molecular mass of the type I tropocollagen may be estimated as high as 3×10^5 Da by using a mean value of 100 Da per amino acid

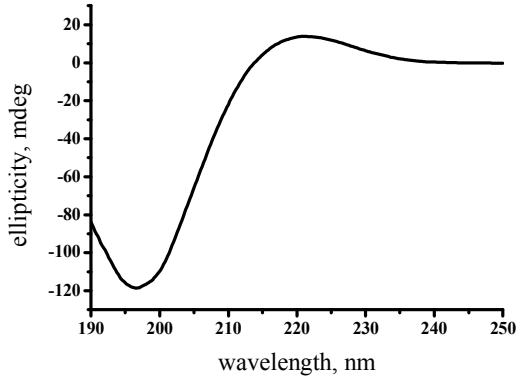

Fig. 2 UV-CD spectrum of CI in solution of 10^{-2}M HCl at room temperature (24^{0}C). Collagen concentration – 0.10%.

residue mass. The experimentally determined value of CI molecular mass (3.59×10^5 Da), slightly higher than that estimated from the overall number of amino acid triplets (3×10^5 Da), supports either a small supramolecular association of collagen in solution or an inherent difference between the two methods for molecular mass estimation. Anyway, the value of 3.59×10^5 Da obtained for the average viscosity molecular mass of CI is consistent with the entire integrity of collagen at molecular level.

Purity and molecular mass evaluation of CI by SDS-PAGE

One of the most sensitive approaches to assess the purity of a protein, together with its molecular mass (M), is SDS-PAGE.[74-76] Applying this method to the CI extracted from calfskin led to a pattern of protein bands as illustrated in Fig. 4. Besides the expected bands derived from collagen and displayed onto electropherogram (bands corresponding to the α1 and α2 chains as well as to β bands of two α-chains chemically linked together), there are no any other bands belonging to an unknown protein.[46,47] This is strong evidence for the high purity of CI obtained and investigated in the present study.

Moreover, considering the chain composition of a CI molecule (two α1 and one α2 polypeptide chains),[2,5] SDS-PAGE is a very useful tool to estimate the molecular mass of CI by comparing the relative mobilities (u_r) of the two types of α-chains (see Fig. 4) to those shown on the log-lin type plot M-u_r for an appropriate mixture of calibration references (Fig. 5). All of the estimated

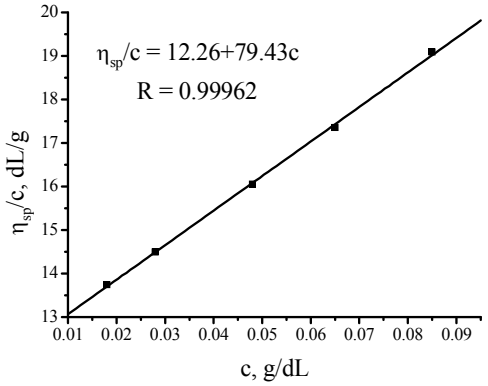

Fig. 3 Concentration dependence of reduced viscosity for CI in 0.15M acetic acid solution at 24.8^{0}C.

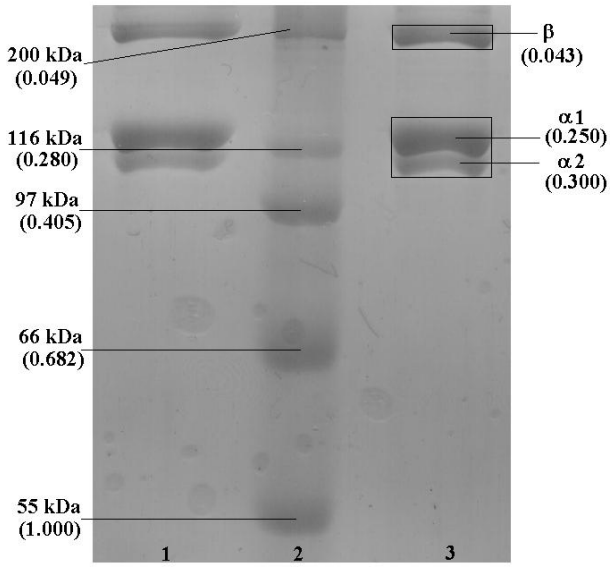

Fig. 4 Electropherogram obtained for CI (lanes 1 and 3) and calibration references (lane 2). Values in parentheses denote conventional relative mobilities calculated with respect to 55 kDa band.

molecular weights were affected by an intrinsic method error of 5%. On the basis of the calibration curve of the α-chains relative mobilities, a CI molecular mass of $(3.53\pm0.18)\times10^5$ Da was obtained. This value is close to that obtained from viscosity measurements (3.59×10^5 Da), which means that collagen is dispersed in the 10^{-2}M HCl solution mostly at molecular level.

Altogether, the data obtained from TEM, UV-CD, viscometry and SDS-PAGE, indicate that CI utilized in the present work is of high purity and molecular integrity and may be considered in monomeric form with some degree of supramolecular aggregates for all the studied samples.

Assessment of the degree of intramolecular crosslinking of CI based on its α-chains composition

One of the most important features related to the heterotrimeric nature of CI molecule is the number ratio between α1 and α2 chains that has to be 2:1. Accordingly, by an adequate processing of the CI electropherogram (SDS-PAGE), it is possible to find out the real number ratio between the two types of α-chains just as they were individually released during the unfolding-denaturation step of CI triple-helix prior to performing electrophoresis. Therefore, a digitally acquired image of the patterned gel after the destaining stage may be processed by means of the Origin 8.1 software facilities. For that purpose, the image of final destained gel was recorded at 1600×1600 dpi resolution in 8-bit grayscale mode (see Fig. 4). This means that each of the pixels on the image may have one of the 2^8=256 shades of gray allowed to be recorded depending of the intensity of gray degree. According to such an assignment, the zero value is ascribed to black colour and 255 – to white colour. Analyzing the total pixelated area framed in Fig. 4, lane 3 allows eventually estimating the corresponding weight ratio between the two kinds of polypeptidic chains (Fig. 6a). In fact, the area of interest consists of 355×306 pixels which correspond to a matrix with 355 columns and 306 rows. As stated, each matrix element is represented by an integer value ranged between 0 and 255, depending upon the gray intensity. By plotting the values of a certain matrix column on the position values (from 0 to 306) of pixels, the graphical estimation of the foregoing weight ratio is straightforward by considering the peak areas corresponding to each of the different α1 and α2 bands.

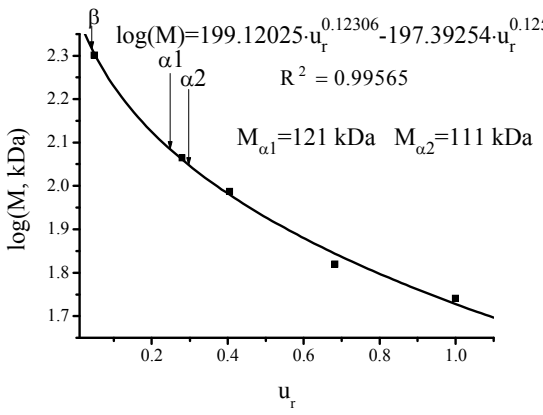

Fig. 5 Calibration curve for the estimation of CI molecular mass. Marker proteins with the relative mobilities inset in Fig. 4 consist of: myosin (rabbit muscle) - 200 kDa, β-galactosidase (E. coli) - 116 kDa, phosphorilase b (rabbit muscle) - 97 kDa, bovine serum albumin – 66 kDa and glutamic dehydrogenase (bovine liver) – 55 kDa.

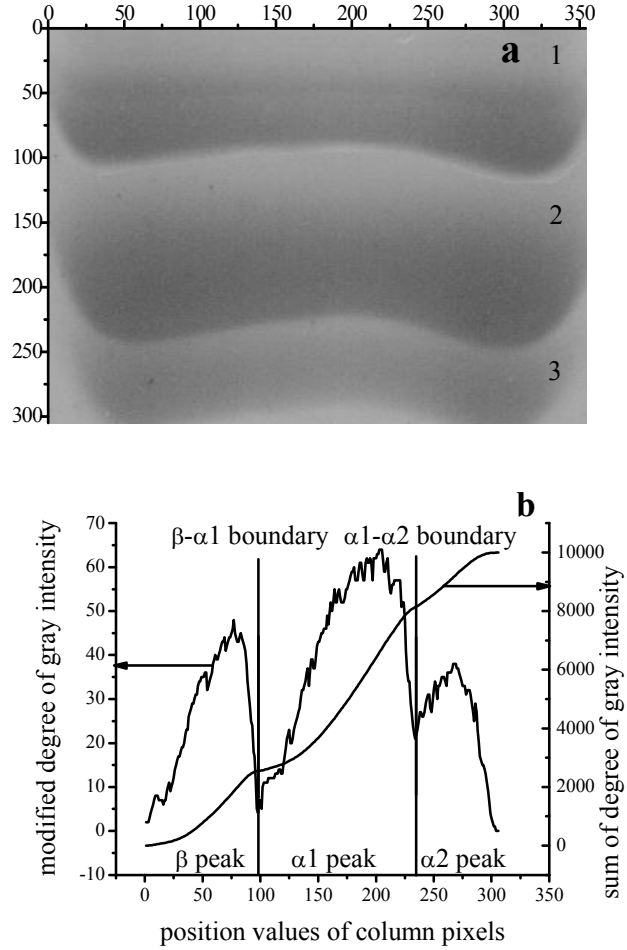

Fig. 6 (a) Pixelated image of the merged bands (1-β band, 2-α1 band, 3-α2 band) framed in Fig. 4 and (b) raw data for gray intensities of pixels – pixels position dependence concerning column 155 from Fig. 6a. The positive peaks are obtained by subtracting the raw data from the maximum intensity value (168) of the specified column.

For illustration, the two peaks originated from column 155 are plotted together with the associated integral curve, as can be seen in Fig. 6b. Thus, the ratio between the area of peak α1 and that of peak α2 is equal to the ratio between the total weight of α1 ($m_{\alpha 1}$) and α2-chains ($m_{\alpha 2}$), respectively and is further equal to 3.01. To obtain a valid value of this ratio from the statistical standpoint, an image region delimited by columns 75 and 277 was selected within which a number of 82 evenly distributed columns were then considered. Based on such a statistical assembly, following the procedure just described, we obtained:

$$\frac{m_{\alpha 1}}{m_{\alpha 2}} = 2.96 \pm 0.15 \quad (3)$$

This quantity is related to the number ratio $n_{\alpha 1}/n_{\alpha 2}$ as follows:

$$\frac{n_{\alpha 1}}{n_{\alpha 2}} = \frac{m_{\alpha 1}}{m_{\alpha 2}} \cdot \frac{M_{\alpha 2}}{M_{\alpha 1}} = 2.72 \pm 0.24 \quad (4)$$

where $n_{\alpha 1}$ and $n_{\alpha 2}$ are the total number of α1-chains with a molecular mass ($M_{\alpha 1}$) of (1.21±0.06)×10^5 Da and α2-chains with a molecular mass ($M_{\alpha 2}$) of (1.11±0.06)×10^5 Da, respectively.

As each of chemically non-crosslinked CI molecule generates three independent α chains during thermally induced denaturation and leads to a number ratio $n_{\alpha 1}/n_{\alpha 2}$ =2, there is most likely that every CI samples contain a mixture of protein molecules: non-crosslinked, crosslinked between α1-α1 chains, crosslinked between α1-α2 chains and crosslinked between all the three α-chains simultaneously. This was partially confirmed by CI SDS-PAGE that exhibited only the migrated bands corresponding to α1-chains, α2-chains and β-fraction (consisting of crosslinked α1-α1 and α1-α2 chains) as shown in Fig. 4 (lanes 1 and 3). Even though γ-fraction (crosslinked α1-α1-α2 chains) might exist, its relative amount could not be estimated due to the too high molecular mass of the CI denatured molecules of γ-fraction that could not migrate through the pores of polyacrylamide gel as the other fractions (β-fraction and α-chains) did during electrophoresis. Practically, to certify the occurrence of γ-fraction, a SDS-PAGE test using a separating gel of 3% was performed and the result was negative. Instead, the migrating bands of β, α1 and α2 fractions of denatured CI (by using the same 6% resolving gel) allowed assessing the extent of intramolecularly crosslinked collagen molecules (α1-α1 and α1-α2 chains) against the non-crosslinked ones.

Unlike the majority of proteins, where the intramolecular chemical crosslinks consist of disulfide bonds which may stabilize their tertiary and/or quaternary structures, the type I collagen is intramolecularly crosslinked through other types of covalent bonds because of the cysteine-free CI primary structure. In this respect, it is unanimously accepted that the intramolecular crosslinks in CI originate from some lysyl residues located in the N-terminal telopeptides belonging to the three adjacent α-chains of the CI triple-helix.[77] This was confirmed by a number of studies performed more than four decades ago.[78-81] Briefly, such a lysyl residue may undergo an oxidative deamination, catalyzed by the lysyl oxidase, yielding the corresponding carbonyl compound (α-amino adipic acid δ-semialdehyde or allysine). In the next step, two neighbouring allysine residues from two N-terminal telopeptide chains give rise to an unsaturated aldehyde (allysine aldol) as a result of an aldol condensation. This two-stage intramolecular crosslinking process eventually involves only joining a pair of α chains together in a single CI molecule, either α1-α1 or α1-α2 chains (β-fraction). Accordingly, this is why the γ-fraction could not be practically detected during the SDS-PAGE tests performed in the present study. Indeed, each of N-terminal telopeptides in bovine type I collagen contains only one residue of lysine (α1 N-telopeptide chain consists of 16 α-amino acid residues: QLSYGYDE**K**STGISVP-α1 helix; α2 N-telopeptide chain has 9 α-amino acid residues: QFDA**K**GGGP-α2 helix),[82] where **K** designates the lysyl residue according to the nomenclature rules for α-amino acids using the one-letter symbol. Depending on the extent of the telopeptides hydrolysis under the pepsin action, some of them may be either completely or partially removed allowing interchain crosslinking as log as the remaining telopeptide chains retain the lysyl residues. As a result, even in the case of CI extracted by limited pepsin digestion, it is possible that intramolecular crosslinks take place via allysine aldol. To a certain extent, this hypothesis was proven earlier by Piez *et al.*[78] for rat skin collagen which showed that the specific lysyl residues involved in intramolecular interchain crosslinking occurring in CI are located near the N-terminus of each α chain of the collagen triple-helix. This corresponds to the eighth residue (numbered from the N-terminus of α1 helix) for the α1 N-telopeptide chains and the fifth residue for the α2 N-telopeptide chains, respectively, for CI extracted from bovine skin.[82] At the same time, the occurrence of the intramolecular crosslinks observed in calfskin CI by SDS-PAGE could be a consequence of an in vitro crosslinking during the extraction procedure or storage in acetic solution. The behaviour aforementioned is entirely consistent with the results of Kang and Gross[81] in their study on intra and intermolecular crosslinking in CI. They stated that the intact rat-tail tendon fibrils contained no aldol crosslinks. Instead, these intramolecular covalent bonds were detected after the rat-tail tendon was solubilised with acetic acid. According to the authors' opinion, that proved the direct influence of the extraction conditions upon the intramolecular crosslinking of CI.

Therefore, following exactly the same algorithm that led to relationships (3) and (4), the weight and number ratios of β-fraction molecules with respect to α2-chains could be expressed as:

$$\frac{m_{\beta}}{m_{\alpha 2}} = 1.41 \pm 0.07 \quad (5)$$

and

$$\frac{n_{\beta}}{n_{\alpha 2}} = \frac{m_{\beta}}{m_{\alpha 2}} \cdot \frac{M_{\alpha 2}}{M_{\beta}} = 0.76 \pm 0.07 \quad (6)$$

where M_{β} = (2.07±0.10) ×10^5 Da is the average molecular mass of β-fraction molecules as resulted from the calibration curve (see Fig. 5) and m_{β} and n_{β} – the total weight and total number of the same kind of molecules, respectively. Supposing that n_u is the percentage of non-crosslinked collagen molecules, $n_{\alpha 1 \alpha 1}$ – percentage of collagen molecules crosslinked intramolecularly between α1-α1 chains and $n_{\alpha 1 \alpha 2}$ – similar quantity for α1-α2 intramolecularly crosslinked (see table 1), a set of three

Table 1 Type I collagen molecules and their descendants resulted during heat-induced denaturation as revealed by SDS-PAGE

Types of CI molecules	CI molecules crosslinked at α1α1α2 chains	CI molecules crosslinked between two α-chains (β-fraction)		non-crosslinked CI molecules
		crosslinked at α1α1	crosslinked at α1α2	
Number of denatured collagenous molecules derived after thermal denaturation of a parent CI molecule	1 (α1α1α2)	2 (α1α1 + α2)	2 (α1α2 + α1)	3 (α1 + α1 + α2)
	γ-fraction	β-fraction		
Number percentage of collagenous molecules migrated in SDS-PAGE	not migrated not existed	$n_{\alpha1\alpha1}$	$n_{\alpha1\alpha2}$	n_u

relationships can be written based on the image processing of the migrated bands on the electropherogram (Fig. 4 and 6a) and neglecting the corresponding uncertainties:

$$n_u + n_{\alpha1\alpha1} + n_{\alpha1\alpha2} = 100 \quad (7)$$

$$\frac{2n_u + n_{\alpha1\alpha2}}{n_u + n_{\alpha1\alpha1}} = 2.72 \quad (8)$$

$$\frac{n_{\alpha1\alpha1} + n_{\alpha1\alpha2}}{n_u + n_{\alpha1\alpha1}} = 0.76 \quad (9)$$

By solving the linear system consisting of equations (7) - (9), a unique tricomponent solution has been derived: $n_u = 56.49$, $n_{\alpha1\alpha1} = 0.76$ and $n_{\alpha1\alpha2} = 42.75$ (in %). This offers a straightforward approach to assess the degree of intramolecular crosslinking of the CI molecules able to migrate during SDS-PAGE after their thermal denaturation. However, this route cannot be precise enough to allow a good estimation of the CI molecules with α1-α1 crosslinks ($n_{\alpha1\alpha1}$ quantity). Therefore, according to the propagation of uncertainties, the estimated final solution consists of: $n_u = 56.49 \pm 8.90$, $n_{\alpha1\alpha1} = 0.76 \pm 10.74$ and $n_{\alpha1\alpha2} = 42.75 \pm 5.99$ (in %). In other words, at least in this case, only the quantities n_u and $n_{\alpha1\alpha2}$ could be satisfactorily estimated. Thus, the original tricomponent solution of equations (7) – (9) was practically reduced to a bicomponent one (due to the small value of $n_{\alpha1\alpha1}$). Even so, the obtained system composition may be considered quite realistic. On the other hand, the preponderant α1-α2 crosslinks compared to the α1-α1 ones, as detected at least in the CI samples extracted from calfskin by pepsin procedure applied in the present study, as well as the corresponding mechanism by which this composition has been brought about need further investigations in the future. This particular experimental approach regarding the assessment of the degree of CI intramolecular crosslinking may find a useful application in detecting the type of soluble collagen carrying its telopeptide ends (even though only partially retained) or completely devoid of these terminal telopeptides as in the case of atelocollagen. The aspect may be of great importance in designing and developing new collagen-based materials, knowing that the CI triple-helix is almost non-immunogen[83] and the C- and N-terminal telopeptides are quite responsible for the collagen antigenicity.[84]

Thermal denaturation of CI in acidic solution (10^{-2}M HCl)

The experimental behaviour experienced by CI during its thermally-induced denaturation was studied by DSC and capillary viscometry.

MicroDSC results

Microcalorimetry investigations performed on the four CI samples (CI acidic solutions of 0.075, 0.100, 0.220 and 0.290% by weight, respectively), each of them at five different heating rates (0.1, 0.2, 0.3, 0.4 and 0.5 $Kmin^{-1}$, respectively), clearly revealed a two-stage denaturation behaviour. The first stage is represented by a minor peak at lower temperatures (peak 1, T_1), while the second major peak located at higher temperatures (peak 2, T_2), is considered as the real denaturation process (corresponding to the helix-unordered state transition) of collagen (Fig. 7).

The thermal evolution of the overall CI denaturation displays a

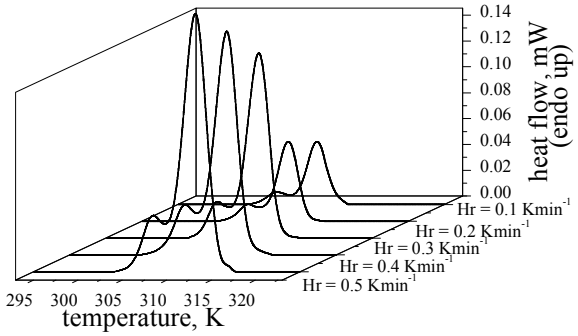

Fig. 7 Heating DSC thermograms (raw data) of 0.290% CI solutions at the indicated heating rates (Hr) after baseline subtraction.

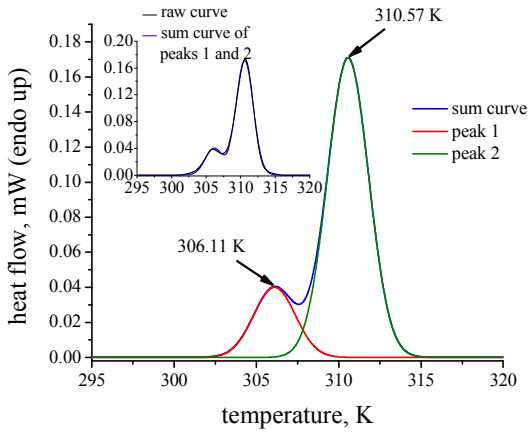

Fig. 8 Peak fitted thermogram (heating) of 0.29% CI solution (Hr = 0.4 $Kmin^{-1}$). The inset exhibits the comparison between the raw thermogram and the sum curve of the peaks 1 and 2 resulted by peak fitting.

shift of both lower- and higher-temperature endotherms by roughly few tenths of a degree Kelvin towards higher temperatures with increasing of the heating rate as shown in Table S1 (ESI). This is a general rule for most processes studied by thermal analysis, similar to those observed in shifting melting temperatures for different types of substances such as natural oils[85] or polymers.[86] In DSC, this is a sign of the activated nature of the denaturation process. For a detailed characterization of the overall denaturation of CI in acidic solutions, the heating DSC thermograms have been processed by using the PeakFit v.4.12 software package. Thus, every DSC thermogram (heating zone, after baseline subtraction) was considered to be a sum of two component curves corresponding to the two endothermic processes as revealed during CI denaturation. Accordingly, the two endothermic peaks were completely separated through a curve decomposition procedure for each of DSC thermogram and, after an extensive trial of built-in peak functions, we used a Gauss area-type function for the peaks shape, with the same FWHM (full width at a half maximum) of both peaks belonging to a certain thermogram. The peak temperatures, relative areas for every pair of peaks and goodness of peak fitting are listed in detail in Table S1 (ESI). Such a curve decomposition example is graphically shown in Fig. 8.

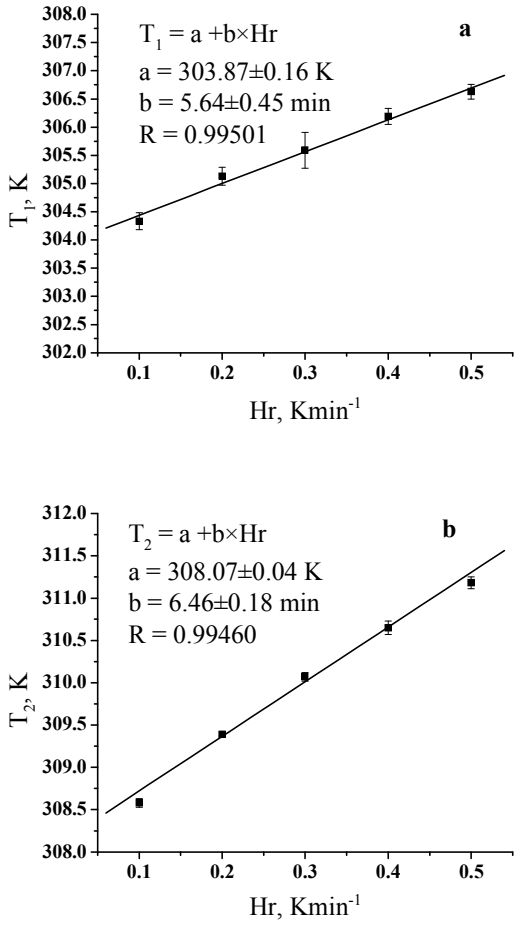

Fig. 9 Concentration-averaged peak temperatures – heating rate dependences and corresponding linear fits for (a) peak 1 and (b) peak 2 of DSC traces of CI solutions.

The two peak temperatures, averaged for all CI concentrations, are plotted in Fig. 9 against the heating rate. There is some weak scatter of T_1 values, while T_2 ones, corresponding to the main denaturation process, are almost concentration-insensitive and fall within experimental scatter. Equilibrium values of the two peak temperatures were evaluated as intercepts of the corresponding linear fits: $(T_{1eq})_{mean}$ = 303.87 K and $(T_{2eq})_{mean}$ = 308.07 K, as "extrapolated to zero heating rate values".

Following the same procedure, the linear dependencies obeyed by the peak temperatures (T_1, T_2) against heating rate were employed in deriving the extrapolated T_{1eq}, T_{2eq} at zero heating rate (see Table S1, ESI). These linear variations T – heating rate are rather different from those found elsewhere,[87] where the apparent temperatures of collagen denaturation were found to vary linearly with the logarithm of heating rates.

Apart from these abovementioned considerations, the most challenging task concerning CI thermally-induced denaturation was to establish the origin of the two endotherms evidenced in DSC thermograms. First of all, based on the data published previously,[38-40] we assigned the peak 2 (major transition) to the denaturation of CI triple-helix. On the other hand, the minor transition (peak 1) was ascribed to either defibrillation of the smaller supramolecular aggregates of CI[39] or partial unfolding of CI triple-helix, supported by the presence of a thermally labile domain, completely devoid of hydroxyproline residues, in the triple-helix structure of CI extracted from either mammalians or fish [40,41,88], or both of them.[39] This is mainly supported by the weight of peak 1 with respect to the overall endotherm (sum of the two peaks).

Averaging the relative areas (in percent) of each type of peaks resulted during DSC experiments, a mean value of 18.6±3.0% has been obtained for peak 1 and 81.4±3.0% for peak 2, respectively (see Table S1, ESI). Following the hypothesis according to which the minor transition might originate from partial unfolding of CI triple-helix, it is known that the thermally more labile domain of triple-helix is of ca. 65 amino acid residues length per α chain in mammalians[40,41] and of probably about 41 amino acid residues for CI extracted from fish.[88] Consequently, the percentage area of peak 1 (compared to the total endotherm) should be ca. 6.5% on average (65 residues of hydroxyproline-free domain represent about 6.5% with respect to the overall length of α chain). But the average weight of peak 1 obtained in this work (18.6±3.0%) is almost 3-fold higher. Therefore, the origin of peak 1 cannot be exclusively associated with such kind of partial denaturation of CI. A reliable solution to this problem was provided by comparison of the molecular mass of CI determined by viscometry (3.59×10^5 Da) and SDS-PAGE (3.53×10^5 Da), on one hand, and that obtained taking into account the overall number of amino acid residues of the entire CI triple-helix (3×10^5 Da),[4,6] on the other hand. Thus, the viscometrically and SDS-PAGE determined molecular mass of CI was higher than 3×10^5 Da (for CI in monomeric form) by 19.7% and 17.7%, respectively. By averaging the two differences, a value of 18.7% resulted, in an excellent agreement with the relative area of peak 1 (18.6%, Table 1S, ESI). However, the experimentally obtained molecular mass of CI (by SDS-PAGE) is in fact an apparent quantity, with a magnitude still depending on the homogeneity of polyacrylamide separating gel, running time or operational temperature. Taking

into account all these arguments, only viscosity average molecular mass of CI could be directly related to the weight of peak 1. Indeed, $\overline{M}_v$ reflects a certain type of average quantity in polydisperse polymers/biopolymers (as in the case of acidic solutions of CI, for example) that is always equal to the real molecular mass of polymer/biopolymer for monodisperse systems. In all our CI samples, the value of $\overline{M}_v$ (3.59×10^5 Da) seems to mirror some degree of supramolecular association of CI in its acidic solutions. Such an extent of supramolecular self assembly exceeds the real molecular mass of CI in monomeric form with about 19.7% that, in turn, falls within the range of the relative area of peak 1 (18.6±3.0%). For exemplification, an apparent polydisperse collagen solution was proposed and briefly discussed (see ESI) to match the polydispersity of the system with the viscosity average molecular mass experimentally determined. Supposing a Gaussian distribution of CI aggregate masses centred at M_0 = 360 kDa (Fig. S1, ESI), a polydispersity profile may be numerically and graphically expressed as in Table S2 (ESI) and Fig. S2 (ESI) respectively. Nevertheless, such a distribution could not be realistic because of the primary mass of CI molecule (300 kDa). Accordingly, any CI supramolecular aggregates should have a mass as multiple of 300 kDa. The simplest composition (consisting of CI in monomeric and dimeric form) suitable for $\overline{M}_v$ = 359 kDa may be derived by considering the expression of this kind of molecular mass:[89]

$$\overline{M}_v = \left(\sum_i w_i M_i^a \right)^{1/a} \quad (10)$$

where w_i and M_i are the weight fraction and the molecular mass corresponding to the i^{th} fraction of a polydisperse system. The quantity a is a constant whose value is 1.80 for CI in 0.15M acetic solution at 24.8^0C as previously shown.[72,73] Based on eq. (10), the weight fraction of CI as monomer (w_1) may be expressed as:

$$w_1 = \frac{M_{CIdimer}^{1.80} - \overline{M}_v^{1.80}}{M_{CIdimer}^{1.80} - M_{CImonomer}^{1.80}} = 0.85 \quad (11)$$

Thus, CI occurs mainly as monomer (85% by weight) and the rest as dimer. This may be a possible profile of CI composition used in this work. The mass fractions of larger supramolecular aggregates (trimers and so on) are practically negligible when the weight of monomer tends to 85% (Table S3). In the particular case of the monomer-dimer-trimer composition of CI, $\overline{M}_v$ of 359 kDa is equivalent with a weight fraction of CI monomer ranges from 85.00 to 93.80% and a weight fraction of trimer almost negligible when w_1 goes down to 85%. The theoretical compositions are given by:

$$w_2 = \frac{w_1 \cdot M_{CImonomer}^a + (1 - w_1) \cdot M_{CItrimer}^a - \overline{M}_v^a}{M_{CItrimer}^a - M_{CIdimer}^a} \quad (12)$$

with:

$$w_1 + w_2 + w_3 = 1 \quad (13)$$

where $w_1 \in [0.8500, 0.9380]$, w_2 (weight of dimer) $\in [0.0012, 0.1476]$, w_3 (weight of trimer) $\in [0.0024, 0.0608]$, $M_{CImonomer}$ = 300 kDa, $M_{CIdimer}$ = 600 kDa, $M_{CItrimer}$ = 900 kDa, and a = 1.80. The corresponding calculated compositions are collected in the Table S3 (ESI). Therefore, in accordance with the experimental data, all the CI acidic solutions contain at least 85% CI in monomeric form and CI self-assembled in small aggregates (most as dimers or/and trimers) via physical interactions to give a molecular mass ($\overline{M}_v$) of 3.59×10^5 Da. The fact that the relative difference between this value and that of CI in monomeric form (19.7%) is in a very good agreement with the relative area of peak 1 on DSC thermogram (18.6%) is strong evidence that allows precisely assigning the origin of the minor transition (peak 1) to a defibrillation process of the CI small aggregates.

Concerning the overall and decomposed thermal effects recorded during DSC experiments on CI acidic solutions, their values are roughly of the same magnitudes as those reported previously on CI in aqueous media.[28,36,38,39,88] Moreover, the values of enthalpy changes of the major endothermic transition (peak 2), which was ascribed to the real denaturation of CI triple-helix, ranged around the theoretical enthalpy of collagen melting, 5.5 kJmol^{-1}, calculated per mole of amino acid residue by Privalov.[90] These quantities are not shown in Table S1, but they may be easily found by multiplying the value of enthalpy change by the corresponding relative area of peak 2. A particular aspect that deserves supplementary investigations is the concentration-dependence of enthalpy change. As can be seen in Table S1, the value of denaturation enthalpy decreases from 9.89±0.11 kJmol^{-1} for 0.075% CI concentration to 5.09±0.09 kJmol^{-1} for 0.220% CI concentration and then rises up to 7.35±0.13 kJmol^{-1} for 0.229% CI concentration in acidic solution.

Only for comparative purposes, an approximate kinetic evaluation of the activation energy of CI denaturation was carried out. Assuming that CI denaturation is governed by a first-order irreversible process,[91-94] the classical Kissinger method was applied. This relies on the established dependence between peak temperatures (in DSC/DTA experiments) and the corresponding heating rates. Accordingly, the Kissinger equation is given as follows:[95-97]

$$-\ln\left(\frac{Hr}{T_p^2}\right) = \frac{E}{R} \cdot \frac{1}{T_p} + Const \quad (14)$$

where E is the activation energy (in kJmol^{-1}), T_p – peak temperature (in K) and R – gas constant (8.314 kJmol^{-1}K^{-1}). The activation energy values derived from the slopes of linear dependencies shown in Fig. 10 were found to be E_1 = 485±43 kJmol^{-1} (peak 1) and E_2 = 474±41 kJmol^{-1} (peak 2), respectively. Because of the similar attractive interactions (mainly hydrogen bonds) disrupted during minor and major denaturation transition of CI in the specified solutions, it was expected to obtain activation energy values (E_1 and E_2) close to each other. This is indeed the case, as seen in Fig. 10. However, there is some variation and scatter in activation energy values among CI samples of different concentrations (Fig. 11). Whereas the slightly higher values found for the most concentrated sample (0.29%) may be considered within the limits of experimental errors, the E_1 value of the 0.220% CI is clearly an outlier. This

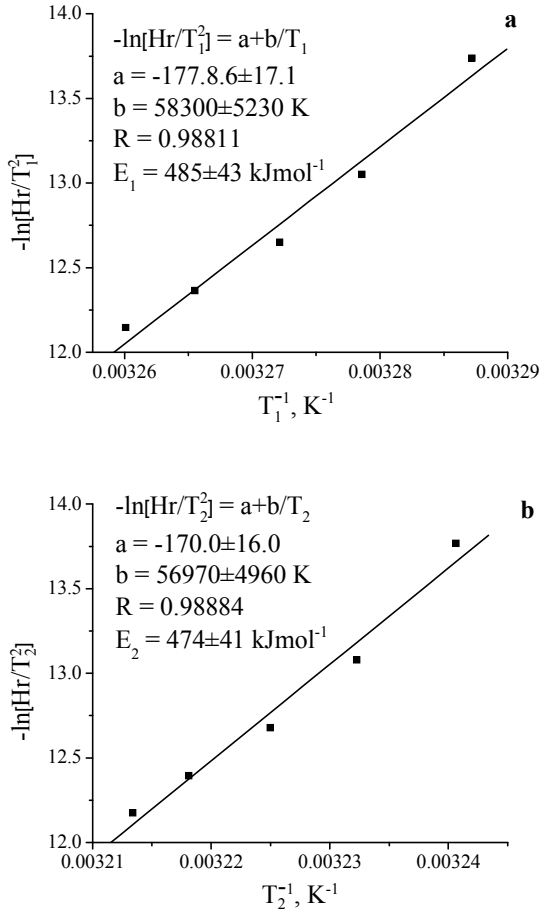

Fig. 10 Kissinger plots of the experimental data associated with (a) peak 1 and (b) peak 2 of DSC thermograms of 0.075% CI solution.

may be due to the failure of PeakFit decomposition of the thermograms pertaining to this peculiar sample. At the same time, such discrepancies may also be due to the failure of the simple Kissinger method to describe the definitely complex processes involved in collagen denaturation.[96] All the above influencing factors may act simultaneously or separately. Anyway, the estimated values of activation energies of denaturation for CI in acidic (10^{-2}M HCl) solution agree fairly well with values reported for thermal denaturation (in water) of CI from rat tendon[92] – ca. 520 kJmol^{-1} or from bovine Achilles tendon[96] – ca. 380 kJmol^{-1}.

Another significant feature revealed by experimental data shown in Table S1 consists of peak temperatures, the most important of which is T_2 for the considerations to come. In this respect, regardless of both the heating rates and CI concentrations, all T_2 values were significantly lower than physiological temperature of the living body as source of collagen extraction. These temperatures increase with heating rate (Fig. 9b), the lowest T_2s being those corresponding to the extrapolated equilibrium temperatures of denaturation, T_{2eq}s. For simplicity and clarity, CI studied in this paper was extracted from calfskin. This animal species, in healthy state, is characterized by an average body temperature of 38.3^{0}C (beef cow) or 38.6^{0}C (dairy cow),[98] higher than those experimentally obtained for thermal denaturation of CI in its acidic solutions. Despite this

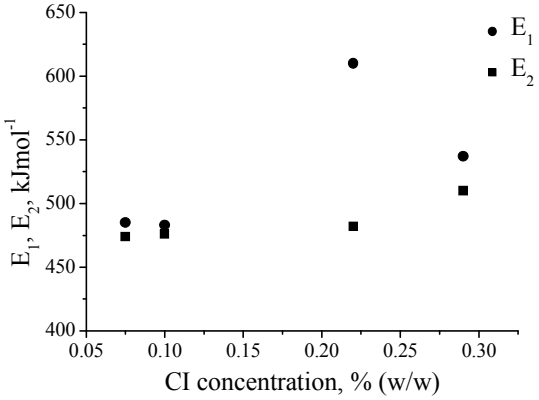

Fig. 11 Variation of simple Kissinger values of the activation energies obtained for the investigated samples against CI concentration.

apparent discrepancy, according to which in living animals CI would be unstable at body temperature, it is important to specify that the majority of CI, secreted by the cells into the extracellular matrix as procollagen (subsequently transformed into the mature collagen molecules), starts to self-assemble into fibrillar structures.[63] These supramolecular fibrils are the key feature of CI state within the extracellular matrix of the connective tissues for a quite long time. Such fibrillar self-assemblies clearly enhance thermal stability of CI by a tight confinement of collagen molecules in fibres that prevent triple-helices to gain as much entropy as in solution and eventually unfold at lower temperatures.[26,87] According to the MicroDSC and the viscosity data (molecular mass evaluation), the obvious conclusion is that the studied acidic solutions of CI exhibit a certain degree of polydispersity (as reflected by the existence of peak 1) within a general picture whereby collagen is mainly dispersed at molecular scale (acidic solution of collagen in monomeric form). This image is in excellent agreement to the experimental results offered by TEM and UV-CD for the same systems.

Capillary viscometry data on CI denaturation

The viscosity data recorded at different temperatures during CI denaturation in acidic solutions revealed only one-step irreversible process associated with helix-unordered state transition. Although capillary viscometry is not sensitive enough to detect the pre-transition stage (corresponding to peak 1 in DSC experiments), the method is quite accurate in monitoring the main transition associated with CI denaturation. Thus, the CI denaturation temperatures (T_D) were determined from the reduced viscosity - temperature plots by fitting the experimental data with a Boltzmann type function for reverse sigmoid:[99]

$$\eta_{red} = (\eta_{red})_{min} + \frac{(\eta_{red})_{max} - (\eta_{red})_{min}}{1 + e^{\frac{T - T_D}{b}}} \quad (15)$$

where $(\eta_{red})_{min}$ and $(\eta_{red})_{max}$ are the lowest and the highest fitted values of the reduced viscosities measured for collagen solutions, T – absolute temperature, T_D – abscissa of the inflexion point taken to be CI denaturation temperature and b – a parameter related to the steepness of sigmoid. Accordingly, T_D value (equivalent to T_2 on DSC thermograms) for 0.075% CI solution was found to be 308.0±0.1 K as can be seen in Fig. 12a. The

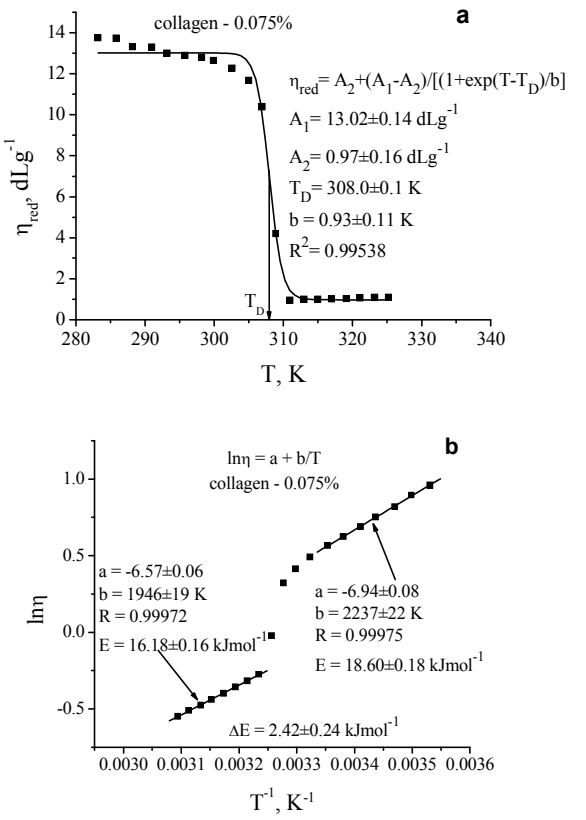

Fig. 12 Suitable viscosity-temperature plots for determining (a) denaturation temperature and (b) activation energy of viscous flow for acidic solution of 0.075% CI.

same value of T_D was obtained for the CI solutions of 0.100 and 0.220% (Fig. S4a and S5a) and a very close value of 307.9±0.1 K was obtained for 0.290% CI solution (Fig. S6a). It is noteworthy that all T_D values viscometrically found are closer to T_{2eq}s than to T_2s (see Table S1, ESI). This is due most likely to the thermostating time of 30 min that led to T_D values much closer to the equilibrium values of T_2 resulted from DSC.

According to Mandal *et al.*,[100,101] the viscosity data are valuable in estimating both the activation energy of viscous flow for the studied CI solutions and enthalpy change of CI denaturation. This approach relies on the Eyring's equation on the influence of temperature upon viscosity of a liquid:[102,103]

$$\eta = \frac{N_A \cdot h}{V} \cdot e^{\frac{\Delta G^*}{RT}} \qquad (16)$$

or, after taking logarithms:

$$\ln \eta = \left[\ln\left(\frac{N_A \cdot h}{V}\right) - \frac{\Delta S^*}{R} \right] + \frac{\Delta H^*}{R} \cdot \left(\frac{1}{T}\right) \qquad (17)$$

where N_A is Avogadro's number, h – Planck constant, V - molar volume of the liquid, ΔG*, ΔH*, ΔS* - molar activation free energy, enthalpy and entropy of liquid flow, R – gas constant and T – absolute temperature. Equation (17) was applied to fit the experimental data expressed as lnη vs. inverse temperature to get the activation quantity ΔH* from the slope of semilogarithmic dependencies. Denoting ΔH*=E (molar activation energy of flow), the values of activation energy have been obtained for both the aqueous solution of 10^{-2}M HCl (Fig. S3, ESI) and the acidic CI solutions (Fig. 12b and Fig. S4-6b from ESI). For each of the investigated CI solutions, a pair of activation energies was calculated: one for temperatures below T_D and the other for temperatures above T_D (Fig. 13). Similarly, two activation energies were obtained for the solvent of CI solutions according to the two temperature domains: below and above T_D of collagen in solution.

The activation energies for CI solutions may serve to estimate the denaturation energy (as enthalpy of denaturation) of CI in acidic solution. Thus, the difference in activation energy after and before collagen denaturation (-ΔE) could be considered as a measure of denaturation enthalpy of collagen at a certain concentration in solution, based on some published studies.[100,101] Moreover, these differences were taken to be the denaturation enthalpy of collagen expressed as average enthalpy per mole of aminoacid residue. In this respect, the values obtained by Mandal *et al.*,[100,101] depending on the collagen source and solution concentration, were scattered around the value of 5.5 kJmol^{-1} predicted by Privalov for the enthalpy of collagen melting. Our experimental data do not sustain at all the results abovementioned. Firstly, for the collagen systems studied in this work, the differences between activation energies in denatured and in nondenatured state, respectively, are negative quantities. This is because the activation energies (as molar activation enthalpies) estimated within temperature range below T_D are higher than those at temperatures above T_D. On the other hand, taking into account the opposite differences (ΔE, positive quantity), their values monotonically decrease from 2.42±0.24 kJmol^{-1} for 0.075% CI solution to 0.88±0.27 kJmol^{-1} for 0.290% CI solution (Fig. 13). These results cannot be rationally related with the enthalpy of collagen denaturation and need further investigations. By critical analysis of the viscous flow activation energies obtained during CI denaturation, at least two important aspects deserve to be mentioned:

(a) As general rule, the activation energy of viscous flow for a liquid solution decreases with temperature,[104] excepting the cases

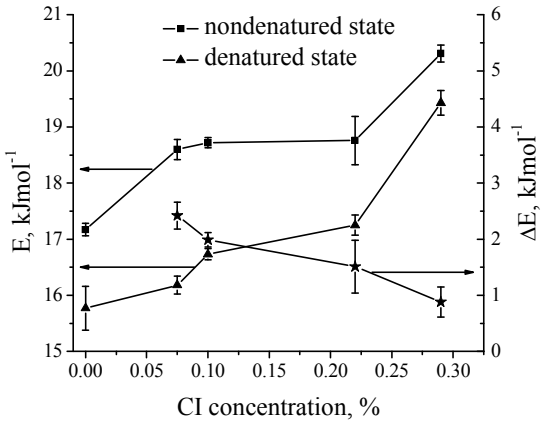

Fig. 13 Evolution of molar activation energy of viscous flow against concentration of CI solutions in nondenatured and denatured state of collagen.

when their viscosity increases with increasing temperature. The viscosity data of CI solutions clearly follow this tendency.

(b) Unlike a pure and simple liquid, a primary viscous flow event in a macromolecular solution implies a movement of a kinetic unit belonging to a macromolecule to an equilibrium position to the nearest neighbouring hole of the liquid system. The stronger the immobilization of the kinetic unit into the macromolecule, the higher the energy barrier (activation energy) required for viscous flow. Accordingly, the activation energy associated to the non-denatured collagen (triple-helical arrangement) has to be higher than that for the collagen in its denatured state (much more flexible at molecular level compared to the triple-helix). Applying Eyring's equation on our experimental data revealed such a feature as can be seen in Fig. 12b and Fig. S4-6b (ESI).

Noteworthy, the viscosity data (activation energy of viscous flow) reported by Mandal *et al*.[100,101] on denaturation process of some collagens are conflicting with the data presented here on CI extracted from calfskin. These facts show that the method of capillary viscometry has to be used with caution, especially in attempting to estimate thermodynamic parameters associated with a denaturation process of protein in solution.

Conclusions

The type I collagen extracted from calfskin and investigated in the present paper showed a native molecular integrity and a conformation of triple-helix as resulted from TEM (molecular shape and length), UV-CD (specific value of Rpn together with the peculiar features of UV-CD spectrum) and capillary viscometry (molecular mass). The high purity of CI in its acidic solutions was assessed by both hydroxyproline content assay and SDS-PAGE. Moreover, by means of SDS-PAGE and subsequent image processing, the occurrence of intramolecular crosslinks was proved, especially between α1 and α2 chains. This type of crosslinks (allysine aldol) might take place as a result of the incomplete removing of some telopeptides during pepsin extraction step of collagen and, after that, during collagen storage in acidic solution. Such a particular way in assessing the existence of possible CI intramolecular crosslinks may serve as useful tool in testing the presence (even partially) of terminal telopeptides of soluble collagens intended for designing and producing some biomaterials. On the other hand, the ultra-sensitive MicroDSC method offered the means to clarify the intimate origin of the two endothermic transitions appeared in the course of CI denaturation in acidic solution. Thus, the equilibrium peak temperatures of the endotherms were located about 30.5-30.8^{0}C for the minor transition (peak 1) and 34.8-35.0^{0}C for the major transition (peak 2), respectively. By correlating the relative areas of the two peaks and taking into account the value of CI molecular mass (359 kDa, viscometrically determined) compared to that of CI in monomeric form (300 kDa), it was possible to precisely ascribe the first peak to defibrillation of the supramolecular aggregates of CI into its individual molecules and the second peak to the real denaturation transition of the native conformation (triple-helix) of collagen. In this respect, the enthalpy values associated to the helix-unordered state transition (peak 2) fall within the range of the theoretical enthalpy of collagen melting (5.5 kJ per mole of amino acid residue) predicted by Privalov. The denaturation temperatures of CI expressed in terms of equilibrium temperatures of peak 2 were fully confirmed by the denaturation data obtained by capillary viscometry. Even though the estimated denaturation equilibrium temperatures for CI acidic solutions are below the body temperature of the mammalian source, the "in vivo" fibrillar state of collagen, as it occurs into the extracellular matrix, prevents the observed thermally induced "in vitro" denaturation tendency.

Acknowledgements

This work was partially supported by an internal grant of the University of Bucharest, project number 587/2014.

Notes and references

[a] *Department of Physical Chemistry, University of Bucharest, 4-12 Regina Elisabeta Blvd., Bucharest 030018, Romania, e-mail: micutz@gw-chimie.math.unibuc.ro*
[b] *Department of Inorganic Chemistry, University of Bucharest, 23 Dumbrava Rosie St., Bucharest 020464, Romania*
[c] *Institute of Physical Chemistry "Ilie Murgulescu", Romanian Academy, Spl. Independenţei 202, Bucharest 060021, Romania*
[d] *National Institute of Materials Physics, 105 Atomiştilor St., Măgurele-Bucharest 077125, Romania*

† Electronic Supplementary Information (ESI) available: DSC data for CI in acidic solutions (peak temperatures, relative peak area, enthalpy changes), calculated polydispersity and compositions of CI in the studied solutions, capillary viscometry data (plots) on thermal denaturation of CI in HCl solution of 10^{-2}M. See DOI: 10.1039/b000000x/

1 M.D. Shoulders and R.T. Raines, *Annu. Rev. Biochem.*, 2009, **78**, 929.
2 D.J.S. Hulmes, *Collagen diversity, synthesis and assembly*, in P. Fratzl (Ed.) *Collagen. Structure and mechanics*, Springer Science+Business Media, LLC, New York, 2008, pp. 15-47.
3 K.E. Kadler, C. Baldock, J. Bella, and R.P. Boot-Handford, *J. Cell. Sci.*, 2008, **120**, 1955.
4 J. Engel, and H.P. Bächinger, *Top. Curr. Chem.,* 2005, **247**, 7.
5 K.E. Kadler, D.F. Holmes, J.A. Trotter, and J.A. Chapman, *Biochem. J.*, 1996, **316**, 1.
6 D.E. Birk, and P. Bruckner, *Top. Curr. Chem.*, 2005, **247**, 185.
7 J.R. Harrisa, A. Soliakov, and R.J. Lewisa, *Micron*, 2013, **49**, 60.
8 J.-H. Bradt, M. Mertig, A. Teresiak, and W. Pompe, *Chem. Mater.*, 1999, **11**, 2694.
9 A. Yokoyama, M. Gelinsky, T. Kawasaki, T. Kohgo, U. König, W. Pompe, and F. Watari, *J. Biomed. Mater. Res. B Appl. Biomater.*, 2005, **75B**, 464.
10 S. Yunoki, E. Marukawa, T. Ikoma, S. Sotome, H. Fan, X. Zhang, K. Shinomiya, and J. Tanaka, *J. Mater. Mater. Med.*, 2007, **18**, 2179.
11 M. Gelinsky, P.B. Welzel, P. Simon, A. Bernhardt, and U. König, *Chem. Eng. J.*, 2008, **137**, 84.
12 N. Nassif, F. Gobeaux, J. Seto, E. Belamie, P. Davidson, P. Panine, G. Mosser, P. Fratzl, and M.-M.G. Guille, *Chem. Mater.*, 2010, **22**, 3307.
13 D.N. Zeiger, W.C. Miles, N. Eidelman, and S. Lin-Gibson, *Langmuir*, 2011, **27**, 8263.
14 S. Heinemann, C. Heinemann, M. Jäger, J. Neunzehn, H.P. Wiesmann, and T. Hanke, *ACS Appl. Mater. Interfaces.*, 2011, **3**, 323.
15 F.J. O'Brien, B.A. Harley, I.V. Yannas, and L. Gibson, *Biomaterials*, 2004, **25**, 1077.
16 F.J. O'Brien, B.A. Harley, I.V. Yannas, and L. Gibson, *Biomaterials*, 2005, **26**, 433.
17 Y.-J. Hwang, J. Granelli, and J. Lyubovitsky, *ACS Appl. Mater. Interfaces.*, 2012, **4**, 261.
18 H.-J. Lee, S.-H. Ahn, and G.H. Kim, *Chem. Mater.*, 2012, **24**, 881.
19 H. Hosseinkhani, Y. Hiraoka, C.-H. Li, Y.-R. Chen, D.-S. Yu, P.-D. Hong, and K.-L. Ou, *ACS Chem. Neurosci.*, 2013, **4**, 1229.
20 S.S. Rao, J. DeJesus, A.R. Short, J.J. Otero, A. Sarkar, and J.O. Winter, *ACS Appl. Mater. Interfaces.*, 2013, **5**, 9276.

21 W.W. Leow, and W. Hwang, *Langmuir*, 2011, **27**, 10907.
22 A. Tenboll, B. Darvish, W. Hou, A.-S. Duwez, S.J. Dixon, H.A. Goldberg, B. Grohe, and S. Mittler, *Langmuir*, 2010, **26**, 12165.
23 Q. Nahar, D.M.L. Quach, B. Darvish, H.A. Goldberg, B. Grohe, and S. Mittler, *Langmuir*, 2013, **29**, 6680.
24 A.I. Brown, L. Kreplak, and A.D. Rutenberg, *Soft Matter.*, 2014, **10**, 8500.
25 C. Jones, L. Liang, D. Lin, Y. Jiao, and B. Sun, *Soft Matter.*, 2014, **10**, 8855.
26 C.A. Miles, and M. Ghelashvili, *Biophys. J.*, 1999, **76**, 3243.
27 G. Shanmugam, and P.L. Polavarapu, *Chirality*, 2009, **21**, 152.
28 P. Budrugeac, and A. Cucos, *Thermochim. Acta.*, 2013, **565**, 241.
29 R. Schweitzer-Stenner, *Mol. Biosyst.*, 2012, **8**, 122.
30 M.L. Tiffany, and S. Krimm, *Biopolymers*, 1969, **8**, 347.
31 A.F. Drake, G. Siligardi, and W.A. Gibbons, *Biophys. Chem.*, 1988, **31**, 143.
32 A.L. Cortajarena, G. Lois, E. Sherman, C.S. O'Hern, L. Regan, and G. Haran, *J. Mol. Biol.*, 2008, **382**, 203.
33 R.K. Dukor, and T.A. Keiderling, *Biopolymers*, 1991, **31**, 1747.
34 B. Bochicchio, and A.M. Tamburro, *Chirality*, 2002, **14**, 782.
35 A.A. Adzhubei, M.J.E. Sternberg, and A.A. Makarov, *J. Mol. Biol.*, 2013, **425**, 2100.
36 E.I. Tiktopulo, and A.V. Kajava, *Biochemistry*, 1998, **37**, 8147.
37 C.C. Danielsen, *Biochem. J.*, 1984, **222**, 663.
38 C. Mu, D. Li, W. Lin, Y. Ding, and G. Zhang, *Biopolymers*, 2007, **86**, 282.
39 Y. Liu, L. Liu, M. Chen, and Q. Zhang, *J. Biomol. Struct. Dyn.*, 2013, **31**, 862.
40 L. He, C. Mu, D. Li, and W. Lin, *Thermochim. Acta.*, 2012, **548**, 1.
41 C.A. Miles, and A.J. Bailey, *Proc. Indian. Acad. Sci.*, 1999, **111**, 71.
42 L. Vitagliano, R. Berisio, R. Mazzarella, and A. Zagari, *Biopolymers*, 2001, **58**, 459.
43 K. Mizuno, T. Hayashi, D.H. Peyton, and H.P. Bächinger, *J. Biol. Chem.*, 2004, **279**, 38072.
44 A. Persikov, J.A.M. Ramshaw, and B. Brodsky, *J. Biol. Chem.*, 2005, **280**, 19343.
45 Z. Deyl, I. Mikšík, and A. Eckhardt, *J. Chromatogr. B.*, 2003, **790**, 245.
46 Z. Zhang, W. Liu, D. Li, and G. Li, *Biosci. Biotechnol. Biochem.*, 2007, **71**, 2057.
47 S. Nalinanon, S. Benjakul, W. Visessanguan, and H. Kishimura, *Food Chem.*, 2007, **104**, 593.
48 A.P. Mould, D.F. Holmes, K.E. Kadler, and J.A. Chapman, *J. Ultrastruct. Res.*, 1985, **91**, 66.
49 K.E. Kadler, and J.A. Chapman, *Ann. N. Y. Acad. Sci.*, 1985, **460**, 456.
50 D.L. Broek, J. Madri, E.F. Eikenberry, and B. Brodsky, *J. Biol. Chem.*, 1985, **260**, 555.
51 N.P. Morris, D.R. Keene, R.W. Glanville, H. Bentz, and R.E. Burgeson, *J. Biol. Chem.*, 1986, **261**, 5638.
52 F.W. Kotch, and R.T. Raines, *Proc. Natl. Acad. Sci.*, 2006, **103**, 3028.
53 M. Micutz, T. Staicu, M. Leca, and C. Ghica, *Rev. Roum. Chim.*, 2009, **54**, 1077.
54 U.K. Laemmli, *Nature*, 1970, **277**, 680.
55 N.Yu. Ignat'eva, N.A. Danilov, S.V. Averkiev, M.V. Obrezkova, V.V. Lunin, and E.N. Sobol, *J. Anal. Chem.*, 2007, **62**, 51.
56 L.J. Bonifer, and G.W. Froning, *J. Food Sci.*, 1996, **61**, 895.
57 P. Kittiphattanabawon, S. Benjakul, W. Visessanguan, T. Nagai, and M. Tanaka, *Food Chem.*, 2005, **89**, 363.
58 V.T. Popa, and E. Segal, *J. Therm. Anal. Cal.*, 2002, **69**, 149.
59 V.T. Popa, *Rev. Roum. Chim.*, 2003, **48**, 987.
60 D.C. Zaharia, C. Iancu, A.T. Steriade, A.A. Muntean, O. Balint, V.T. Popa, M.I. Popa, and M.A. Bogdan, *BMC Microbiology*, 2010, **10**, 322.
61 D.C. Zaharia, A.A. Muntean, M.G. Popa, A.T. Steriade, O. Balint, R. Micut, C. Iftene, I. Tofolean, V.T. Popa, C. Baicus, M.A. Bogdan, and M.I. Popa, *BMC Microbiology*, 2013, **13**, 171.
62 D.J. Prockop, and K.I. Kivirikko, *Annu. Rev. Biochem.*, 1995, **64**, 403.
63 T. Koide, and K. Nagata, *Top. Curr. Chem.*, 2005, **247**, 85.
64 L. Bozec, and M. Horton, *Biophys. J.*, 2005, **88**, 4223.
65 R. Usha, and T. Ramasami, *Thermochim. Acta.*, 2004, **409**, 201.
66 Z.K. Zhang, G.Y. Li, and B. Shi, *J. Soc. Leather Technol. Chem.*, 2006, **90**, 23.
67 Y. Feng, G. Melacini, J.P. Tualane, and M. Goodman, *J. Am. Chem. Soc.*, 1996, **118**, 10351.
68 D. Barth, A.G. Milbradt, C. Renner, and L. Moroder, *Chembiochem.*, 2004, **5**, 79.
69 R. Gayatri, A.K. Sharma, R. Rajaram, and T. Ramasami, *Biochem. Biophys. Res. Commun.*, 2001, **283**, 229.
70 M.L. Huggins, *J. Am. Chem. Soc.*, 1942, **64**, 2716.
71 I. Teraoka, *Polymer solutions*, John Wiley & Sons, New York, 2002, p. 216.
72 T. Nishihara, and P. Doty, *Proc. Natl. Acad. Sci.*, 1958, **44**, 411.
73 K. Pietrucha, *J. Radioanal. Nucl. Chem.*, 1991, **149**, 317.
74 A.L. Shapiro, E. Viñuela, and J.V. Maizel Jr., *Biochem. Biophys. Res. Commun.*, 1967, **28**, 815.
75 K. Weber, and M. Osborn, *Proteins and sodium dodecyl sulfate: molecular weight determination on polyacrylamide gels and related procedures*, in H. Neurath, and R.L. Hill (Eds) *The proteins*, volume I, third edition, Academic Press, Inc., New York, 1975, pp. 180-221.
76 D.L. Nelson, and M.M. Cox, *Lehninger principles of biochemistry*, fourth edition, W.H. Freeman & Company, New York, 2004, pp. 92-96.
77 R.S. Bhatnagar, *Collagen*, in: G.P. Talwar, and L.M. Srivastava (Eds.), *Textbook of biochemistry and human biology, Third edition,* Prentice-Hall of India, New Delhi, 2003, pp. 85-86.
78 P. Bornstein, A.H. Kang, and K.A. Piez, *Proc. Natl. Acad. Sci. USA.*, 1966, **55**, 417.
79 M. Rojkind, L. Rhi, and M. Aguirre, *J. Biol. Chem.*, 1968, **243**, 2266.
80 K. Deshmukh, and M.E. Nimni, *J. Biol. Chem.*, 1969, **244**, 1787.
81 A.H. Kang, and J. Gross, *Proc. Natl. Acad. Sci.*, 1970, **70**, 1307.
82 J.P. Malone, A. George, and A. Veis, *Proteins*, 2004, **54**, 206.
83 J. Risteli, and L. Risteli, *Products of bone collagen metabolism*, in M.J. Seibel, S.P. Robins, and J.P. Bilekizian (Eds) *Dynamics of bone and cartilage metabolism*, Academic Press, San Diego, 2006, p. 399.
84 A.K. Linn, I.V. Yannas, and W. Bonfield, *J. Biomed. Mater. Res. Part B: Appl.Biomater.*, 2004, **71B**, 343.
85 C.P. Tan, and Y.B. Che Man, *Photochem. Anal.*, 2002, **13**, 129.
86 K. Cho, F. Li, and J. Choi, *Polymer*, 1999, **40**, 1719.
87 E. Leikina, M.V. Mertts, N. Kuznetsova, and S. Leikin, *Proc. Natl. Acad. Sci.*, 2002, **99**, 1314.
88 D. Hickman, T.J. Sims, C.A. Miles, A.J. Bailey, M. de Mari, and M. Koopmans, *J. Biotech.*, 2000, **79**, 245.
89 C. Tanford, *Physical chemistry of macromolecules*, John Wiley & Sons, Inc, New York, 1961, pp. 145-50.
90 P.L. Privalov, *Microcalorimetry of macromolecules. The physical bases of biological structures*, John Wiley & Sons, Inc, New Jersey, 2012, p. 145.
91 C.A. Miles, *Int. J. Biol. Macromol.*, 1993, **15**, 265.
92 C.A. Miles, T.V. Burjanadze, and A.J. Bailey, *J. Mol. Biol.*, 1995, **245**, 437.
93 N.T. Wright, and J.D. Humphrey, *Annu. Rev. Biomed. Eng.*, 2002, **4**, 109.
94 M. Weijers, P.A. Barneveld, M.A.C. Stuart, and R.W. Visschers, *Protein Sci.*, 2003, **12**, 2693.
95 H.E. Kissinger, *Anal. Chem.*, 1957, **29**, 1702.
96 S. Vyazovkin, L. Vincent, and N. Sbirrazzuoli, *Macromol. Biosci.*, 2007, **7**, 1181.
97 P.E. Sánchez-Jiménez, J.M. Criado, and L.A. Pérez-Maqueda, *J. Therm. Anal. Cal.*, 2008, **94**, 427.
98 W.O. Reece, *Functional anatomy and physiology of domestic animals*, Fourth ed. Wiley-Blackwell, Ames, Iowa, 2009, p. 422.
99 M. Micutz, T. Staicu, D. Sulea, M. Leca, and C. Ghica, *Rev. Roum. Chim.*, 2010, **55**, 501.
100 A.B. Mandal, D.V. Ramesh, and S.C. Dhar, *Eur. J. Biochem.*, 1987, **169**, 617.
101 C. Rose, M. Kumar, and A.B. Mandal, *Biochem. J.*, 1988, **249**, 127.
102 H. Eyring, *J. Chem. Phys.*, 1936, **4**, 283.
103 R.B. Bird, W.E. Stewart, and E.N. Lightfoot, *Transport phenomena*. Second edition, John Wiley & Sons, Inc, New York, 2002, pp. 29-31.

104 K. Monkos, *Gen. Physiol. Biophys.*, 2011, **30**, 121.